

Effect of cholesterol on the hydration properties of ester and ether lipid membrane interphases

H.A. Pérez, L.M. Alarcón, A.R. Verde, G.A. Appignanesi, R.E. Giménez, E.A. Disalvo, M.A. Frías



PII: S0005-2736(20)30332-1

DOI: <https://doi.org/10.1016/j.bbamem.2020.183489>

Reference: BBAMEM 183489

To appear in: *BBA - Biomembranes*

Received date: 2 May 2020

Revised date: 28 September 2020

Accepted date: 29 September 2020

Please cite this article as: H.A. Pérez, L.M. Alarcón, A.R. Verde, et al., Effect of cholesterol on the hydration properties of ester and ether lipid membrane interphases, *BBA - Biomembranes* (2018), <https://doi.org/10.1016/j.bbamem.2020.183489>

This is a PDF file of an article that has undergone enhancements after acceptance, such as the addition of a cover page and metadata, and formatting for readability, but it is not yet the definitive version of record. This version will undergo additional copyediting, typesetting and review before it is published in its final form, but we are providing this version to give early visibility of the article. Please note that, during the production process, errors may be discovered which could affect the content, and all legal disclaimers that apply to the journal pertain.

EFFECT OF CHOLESTEROL ON THE HYDRATION PROPERTIES OF ESTER AND ETHER LIPID MEMBRANE INTERPHASES.

H.A. Pérez¹, L. M. Alarcón², A. R. Verde², G. A. Appignanesi², R. E. Giménez¹, E. A. Disalvo¹, M.A. Frías¹

¹Applied Biophysics and Food Research Center (Centro de Investigaciones en Biofísica Aplicada y Alimentos, CIBAAL, National University of Santiago del Estero and CONICET) RN 9 - Km 1125, 4206 Santiago del Estero, Argentina.

²Laboratorio de Físicoquímica, INQUISUR, Departamento de Química, Universidad Nacional del Sur (UNS)-CONICET, Av. Alem 1253, 8000 Bahía Blanca, Argentina.

Corresponding author e-mail: marafrias@hotmail.com

Summary: 5194 words and eight (8) Figures

Abstract

Fluorescence spectroscopy and Molecular Dynamics results show that Cholesterol reduces water along the chains in ether lipids by changing the water distribution pattern between tightly and loosely bound water molecules. Water distribution was followed by emission spectra and generalized polarization of 6-dodecanoyl-2-dimethyl aminonaphthalene (Laurdan) inserted in 1,2-dimiristoyl-*sn*-glycero-3-phosphocholine (DMPC) and 1,2-di-*O*-tetradecyl-*sn*-glycero-3-phosphocholine (14:0 Diether PC) membranes. Molecular dynamics simulations indicate that the action of cholesterol could be different in ether PC in comparison to ester PC. In

addition, Cholesterol seems to act “per se” as an additional hydration center in ether lipids.

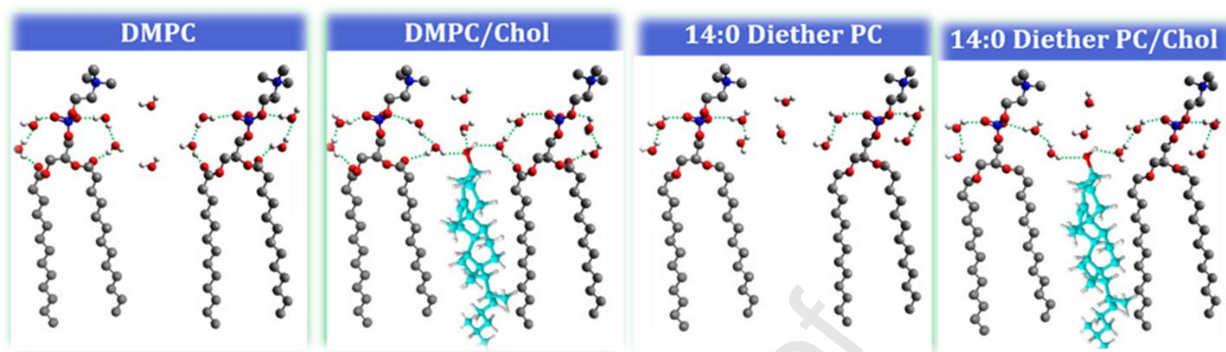
Regardless of the phase state, Cholesterol both in DMPC and 14:0 Diether PC vesicles, changed the distribution of water molecules decreasing the dipole relaxation of the lipid interphase generating an increase in the non-relaxable population. Above 10% Cholesterol/14:0 Diether PC ratio vesicles’ interphase present an environment around Laurdan molecules similar to that corresponding to ester PC.

Keywords: 14:0 Diether PC; DMPC; cholesterol; generalized polarization; hydration; molecular dynamics.

Highlights:

- Cholesterol conforms a new hydration site in membranes lacking carbonyl groups.
- An increase in 14:0 Diether PC polarization is produced at 10 % Chol below T_m not observed in ester PC.
- The transition observed at 10% Chol in 14:0 Diether PC is due to an increase of non relaxable water molecules population.

Graphical Abstract



Abbreviations: DMPC: 1,2-dimyristoyl-*sn*-glycero-3-phosphocholine; 14:0 Diether PC: 1,2-di-O-tetradecyl-*sn* glycero-3-phosphocholine; Laurdan: 6-dodecanoyl-2-dimethyl aminonaphthalene; T_m : Transition temperature; GP: Generalized Polarization; FWHM: full width at half-maximum.

ACKNOWLEDGEMENTS

Funds from ANPCyT (PICT 2015-1111). LMA, GAA, EAD and MAF are members of the permanent research career of CONICET. HAP, ARV and REG are recipients of a fellowship from CONICET (RA).

1. Introduction

It is well known that Cholesterol (Chol) plays a major role in biological membrane functions and ether lipids are involved as plasmalogens in its traffic [1,2].

Therefore, studies in relation to the interaction of Chol and ether lipids in model membranes are pertinent.

Chol affects the properties of the gel and liquid crystalline phases of phosphatidylcholines. In general, it is accepted that it expands the gel phase and compresses the liquid crystalline one decreasing the cooperativity at the transition temperature (T_m) that remains unchanged [3,4]. At high Chol concentrations, the phase transition tends to disappear which denotes that this molecule affects the degree of freedom of the rotational isomers of the acyl chains [5–7].

In addition, the action of Chol has been also related to the hydration state of the lipid membrane. In particular, using Laurdan as a fluorescent probe, the changes of water properties in its immediate adjacencies has been reported. Above the phase transition temperature Chol promotes an increase in generalized polarization (GP) of the membrane, a parameter that is indirectly related to the decrease of water in the membrane phase [7,8].

The decrease in water content has been considered a consequence of the increase in packing by Chol above T_m . However, a recent work has shown that the same shift in GP can be obtained when octanol is deprived of water indicating that no structural change in the phase is required to produce a decrease in GP [9]. In other words, Chol effect modulates the water content of the membrane independently of the packing and Laurdan is an appropriate probe to measure it.

The hydration levels of the lipid membranes can be defined in three regions: water organized around the phosphate groups, the carbonyl groups and the acyl chains.

Molecular Dynamics (MD) studies and interface-selective vibrational sum frequency generation (VSFG) spectroscopy have also detected a population around the choline groups [10].

Moreover, hydration of each of these regions is correlated. The water-phosphate interaction is enhanced when carbonyl groups are absent [11,12]. It has been shown using a combination of fluorescent spectroscopy, FTIR-ATR analysis and monolayer surface pressure/area isotherms that the population of relaxable water molecules is increased in ether in comparison to ester PC [13]. This has been explained by the formation of water bridges between phosphate (PO) and carbonyl (CO) groups of the PCs that hinders the rotational degrees of freedom which are gained when the water molecule is linked only to the PO in the ether lipid [13–15].

It is understood that in the absence of CO groups the hydrogen bonds with the phosphate groups are strengthened [12,16,17]. Thus, the water molecules form with the phosphate a tighter first hydration shell making, in consequence, a looser second hydration shell.

This particular feature of hydration due to the absence of CO groups could be modified by Chol given that it may change the propensity to displace water in processes in which interphases are involved (peptides penetration, fusion, etc.). In this sense, it would be of interest to determine if Chol can be “per se” a hydration site in ether lipids. In order to assess this point the effect of Chol on water distribution in ether PC membranes in comparison to ester PC in the same phase

state was studied using fluorescence properties of Laurdan. The distribution of water and the hydrogen bond populations in each of the conditions assayed were modeled by Molecular Dynamics.

2. Materials and Methods

2.1. Chemicals:

1,2-dimyristoyl-*sn*-glycero-3-phosphocholine (DMPC); 1,2-di-O-tetradecyl-*sn*-glycero-3-phosphocholine (14:0 Diether PC); were purchased from Avanti Polar Lipids Inc. (Alabaster, AL); Cholesterol (Chol) was from Sigma-Aldrich. Purity of lipids and Cholesterol were higher than >99% as checked by FTIR and UV spectroscopies. Laurdan (6-dodecanoyl-2-dimethyl aminonaphthalene) was obtained from Molecular Probes and used without further purification. Chloroform was obtained from Merck and was previously dehydrated with 5 Å molecular sieves during five days. All other chemicals were of analytical grade. All aqueous solutions were prepared with ultrapure water (conductivity = 0.002–0.010 mS cm⁻¹) obtained from an OSMOION 1000 water purification system (APEMA, Buenos Aires, Argentina).

2.2. Samples preparation

Stock solutions of DMPC, 14:0 Diether PC and Laurdan were prepared in Chloroform. Laurdan concentration of the solution was determined by absorption spectrophotometry in the ultraviolet region, at a maximum wavelength of 364 nm

corresponding to an absorptivity coefficient of $20.000 \text{ M}^{-1} \text{ cm}^{-1}$. The final molar ratio Laurdan/lipid was in all cases 1:500 [15,18].

Multilamellar vesicles (MLV's) were prepared following Bangham technique [19]. Vesicles with different Chol/lipid ratio were prepared mixing the appropriate aliquots of Chol and PC stock solutions in chloroform.

LUV's suspensions were prepared by extruding the MLV's suspensions 20 times above T_m through a polycarbonate filter (pore diameter 100 nm). Particle size in the final suspension was determined by dynamic light scattering in a DLS- Horiba nano particle analyzer SZ-100, at 90° with an accuracy $\pm 2\%$ at 25°C [20].

2.3. Fluorescence spectroscopy measurements

Steady-state emission spectra were obtained in a SLM 4800 spectrofluorometer using a 1.0 cm quartz cell in the range of 390–600 nm, equipped with a cell holder controlled by thermostated water. The excitation wavelength was 370 nm with a 2 nm slit. Emission spectra were recorded between 10 to $50^\circ \text{C} \pm 0.1^\circ \text{C}$ in suspensions with an optical density smaller than 0.05 in the range of work given above. Consequently, no correction for the inner filter effect was needed.

Generalized Polarization (GP_{ex}) function was calculated from the emission intensities using the following Equation 1 adapted from Parasassi et al. [15,21–23].

$$GP_{ex} = \frac{I_{440} - I_{480}}{I_{440} + I_{480}} \quad (1)$$

where I_{440} and I_{480} correspond to the emission maxima of Laurdan below and above T_m , respectively.

2.3.1. Spectra decomposition procedure

Fluorescence spectra were fitted using a superposition of two LN mirror symmetric functions using Equation 2 as reported by Bacalum et al. [24].

$$I(\bar{\nu}) = \begin{cases} I_m \exp \left[-\frac{\ln 2}{\ln^2 \rho} \ln^2 \frac{a-\bar{\nu}}{a-\bar{\nu}_m} \right], & \bar{\nu} < a \\ 0, & \bar{\nu} \geq a \end{cases} \quad (2)$$

Where I is the emission intensity, ν is the wavenumber, I_m the maximum intensity, ρ the asymmetry of the function, a the limiting wavenumber and $\bar{\nu}_m$ the peak position. a and ρ are functions of the wavenumber values at half-intensity, $\bar{\nu}_{\max}$ and $\bar{\nu}_{\min}$:

$$p = \frac{\bar{\nu}_m - \bar{\nu}_{\min}}{\bar{\nu}_{\max} - \bar{\nu}_m} \quad a = \bar{\nu}_m + \frac{(\bar{\nu}_{\max} - \bar{\nu}_{\min})\rho}{\rho^2 - 1}$$

$\bar{\nu}_{\max}$ and $\bar{\nu}_{\min}$ are linear functions of $\bar{\nu}_m$ depending on the polarity of the solvent, below 22300 cm^{-1} polar solvents, and above 22300 cm^{-1} for non-polar solvents:

$$\bar{\nu}_{\min}(x) = \begin{cases} -99.4 + 0.966 \times \bar{\nu}_m, & \bar{\nu}_m < 22300 \text{ cm}^{-1} \\ 1150.7 + 0.877 \times \bar{\nu}_m, & \bar{\nu}_m \geq 22300 \text{ cm}^{-1} \end{cases}$$

$$\bar{\nu}_{\max}(x) = \begin{cases} 1688.8 + 0.986 \times \bar{\nu}_m, & \bar{\nu}_m < 22300 \text{ cm}^{-1} \\ -99.3 + 1058 \times \bar{\nu}_m, & \bar{\nu}_m \geq 22300 \text{ cm}^{-1} \end{cases}$$

Following this procedure, the components of Laurdan emission bands in the different conditions can be obtained. The fitting was performed using a script written in Python 3.7 using Pandas and Numpy libraries [25–27]

2.4. Molecular dynamics simulations

The different phospholipid/Chol bilayers were assembled with the CHARMM-GUI Membrane Builder [28]. Pure DMPC and 14:0 Diether PC bilayers were prepared with 64 lipid molecules in each leaflet, and 30% Chol mixed membranes were prepared with 45 phospholipid molecules and 19 Chol molecules in each leaflet. Simulations were performed with AMBER16 simulation package [29] with bond, angle, torsion, and Lennard-Jones parameters from Lipid17 force field [30] taken directly from the General Amber Force Field (GAFF) [31]. Membranes were solvated with TIP3P water molecules along the Z axis with enough molecules to assure the systems were fully hydrated. After membranes were assembled, the full systems were minimized for 10000 steps, the first 5000 steps used the steepest descent method and the remaining steps used the conjugate gradient method [32]. Systems were then heated from 0 K to 100 K using Langevin dynamics [33] for 5 ps at constant volume, with weak restraints on the lipid. Then, the volume was allowed to change freely and the temperature increased to the informed values with a Langevin collision frequency of $\gamma = 1.0 \text{ ps}^{-1}$, and anisotropic Berendsen regulation [34] with a time constant of 2 ps for 100 ps. After 150 ns equilibrium run, a final production was carried out within the NPT (constant number of atoms N, pressure P and temperature T) ensemble. The extent of the trajectories of the production runs was 100 ns for the different systems. SHAKE was activated for hydrogen bonds, using particle mesh Ewald for periodic boundary conditions to treat long-range electrostatics interactions [35] with a 10 \AA cut off and a simulation time step of 2 fs.

3. Results

Figure 1 shows the modification of the full width at half maximum (FWHM) obtained from the normalized Laurdan emission spectra for DMPC (Fig. S1) and 14:0 Diether PC (Fig. S2), below (Part A) and above (Part B) T_m for increasing Chol ratio.

For 14:0 Diether PC below T_m , FWHM decreases abruptly at 10% Chol and an equivalent upward jump is observed above T_m . These discontinuities are not observed in DMPC/Chol mixtures in both states.

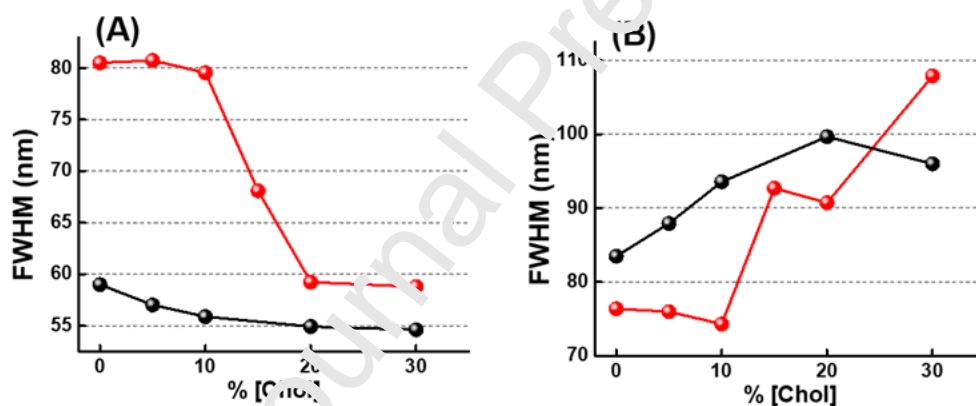


Fig 1: FWHM vs % Chol. (A) 14:0 Diether PC (red symbols) and DMPC (black symbols) below T_m . (B) 14:0 Diether PC (red symbols) and DMPC (black symbols) above T_m .

In order to analyze the effect of Cholesterol on the dipolar relaxation in ester and ether PCs, generalized polarization function (GP_{ex}) was calculated using Equation 1 shown in Materials and Methods.

The striking difference observed in FWHM between DMPC and 14:0 Diether PC below T_m is also noticeable when the GP_{ex} behaviour is analysed (Fig. 2). Part A shows that GP_{ex} values for DMPC are much higher than those for 14:0 Diether PC below T_m and 10% Chol. At this ratio an abrupt increase occurs which is not observed in DMPC. On the other hand, the changes above T_m does not show this transition neither in DMPC nor 14:0 Diether PC (Fig. 2B).

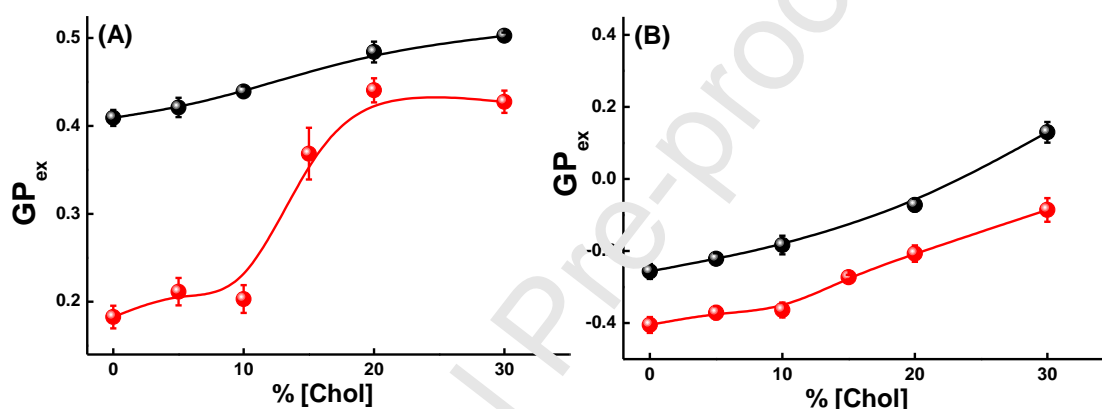


Fig. 2: GP_{ex} values for DMPC (black symbols) and 14:0 Diether PC vesicles (red symbols) at different Chol ratio, below (A) and above (B) T_m .

It has been widely reported that the emission spectrum of Laurdan is a superposition of the non-relaxable and the relaxable emitting states. These two emitting states can be obtained by Log-Normal (LN) decomposition of Laurdan emission fluorescence [24,36]. These emitting states are an indirect measure of water molecules' populations with different rotational degrees of freedom surrounding Laurdan [13,24].

The contributions of these populations were analysed as a function of Chol ratio in DMPC and 14:0 Diether PC below and above T_m using Eq 2 from Materials and Methods and are shown in Fig. 3.

Figure 3A shows the changes in the distributions of relaxable and non-relaxable populations for DMPC below T_m without (part A) and with 20% Chol (part B). In the first case, there is small contributions of relaxable populations which disappear in the presence of Chol (part B). For DMPC the non-relaxable and relaxable populations represent 78% and 22% of the total emission. In the presence of 20% Chol, the non-relaxable and relaxable populations are 100 and 0 % respectively.

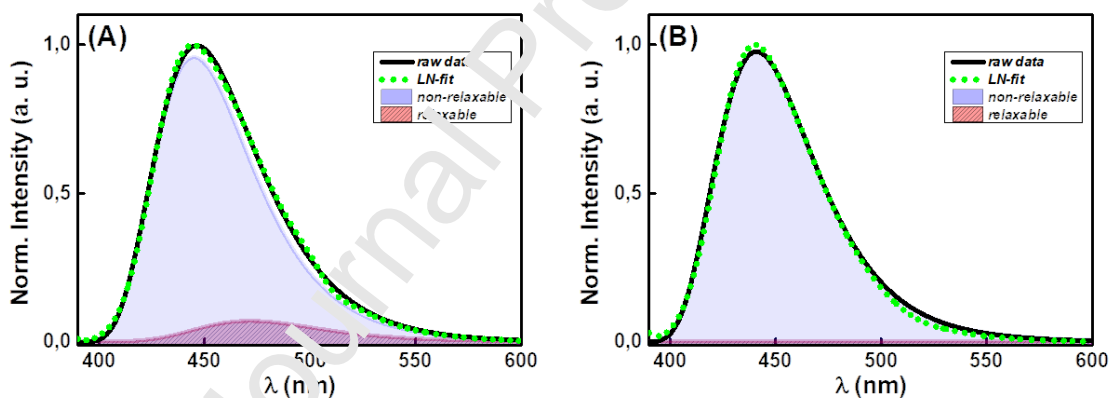


Fig. 3: Decomposition Laurdan spectra below T_m for DMPC (part A) and DMPC/20% Chol (Part B).

On the other hand, in Fig. 4, the effect of Chol on 14:0 Diether PC on relaxable and non-relaxable populations below T_m are shown. In comparison to DMPC, Fig. 4A shows that the relaxable - non relaxable ratio is considerably increased in the ether lipid which is substantially decreased in the presence of Chol (Part B). However,

this ratio is much greater in 14:0 Diether PC/Chol than in DMPC/Chol shown in Fig. 3B.

For 14:0 Diether PC the non-relaxable population contribution decreases 15% with a corresponding increase for the relaxable population. In the presence of 20 % Chol, 14:0 Diether PC restores the contributions to levels similar to DMPC, 79% for non-relaxable and 21% for relaxable populations.

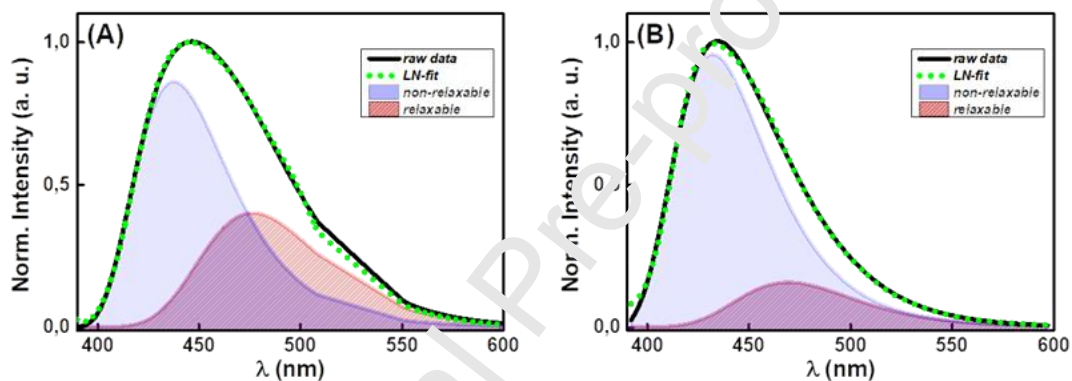


Fig. 4: Deconvolution of Laurdan spectra below T_m for 14:0 Diether PC (Part A) and 14:0 Diether PC/20% Chol (Part B).

Figure 5 resumes the changes in relaxable and non-relaxable populations for 14:0 Diether PC and DMPC below (part A) and above (part B) T_m produced by increasing Chol ratios.

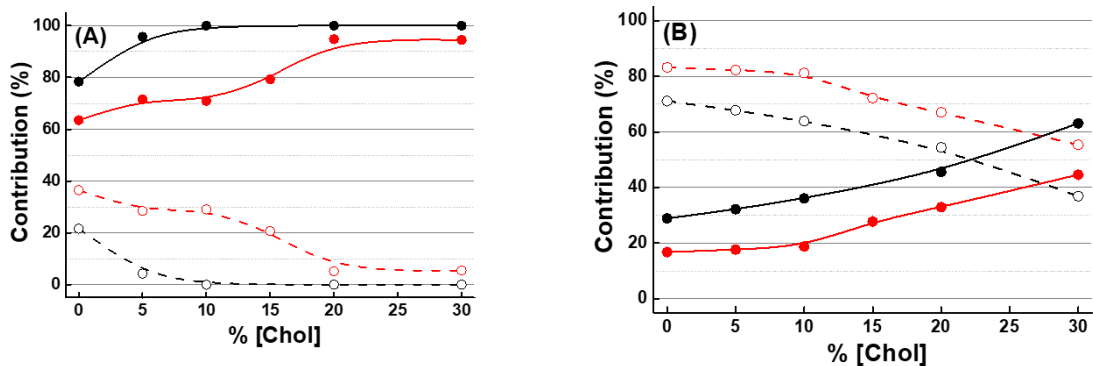


Fig. 5: Percentual Contribution (%) of relaxable and non-relaxable populations depending on Chol ratio in DMPC and 14:0 Diether PC below (A) and above (B) T_m . Filled symbols correspond to DMPC (in black) and 14:0 Diether PC (in red) non-relaxable populations. Empty symbols correspond to DMPC (in black) and 14:0 Diether PC (in red) relaxable populations.

In Figure 5A, the non-relaxable water population in DMPC increases continuously with Chol and reaches saturation at 10% Chol. For 14:0 Diether PC, a slight increase of the non-relaxable population is produced at 5 % Chol. A second and more intense increase is produced between 10 and 20% Chol. This last increase is at the same Chol ratio in which the discontinuities in FWHM and GP_{ex} were observed in previous figures. So, the effect of Chol is qualitatively different in 14:0 Diether PC in comparison to DMPC below T_m . However, above T_m , (Fig. 5B) Chol produces the same decrease in the relaxable water population both for DMPC and 14:0 Diether PC.

The increase of the non-relaxable water populations with Chol parallel to the decrease of relaxable water populations indicates that Chol affects the rotational degrees of freedom of water molecules in a different way in ether and ester PC. A further inspection in regard to the different distributions of water species according

to the kind and number of H-bonds they form with its surroundings for pure DMPC and 14:0 Diether PC was performed by MD.

Below and above T_m (panels A, B, C in Figure 6) and in the presence of Chol (panels D, E, F in Figure 6) the index that classifies water molecules by their number of water-water, water-PO and water-CO hydrogen bonds is shown

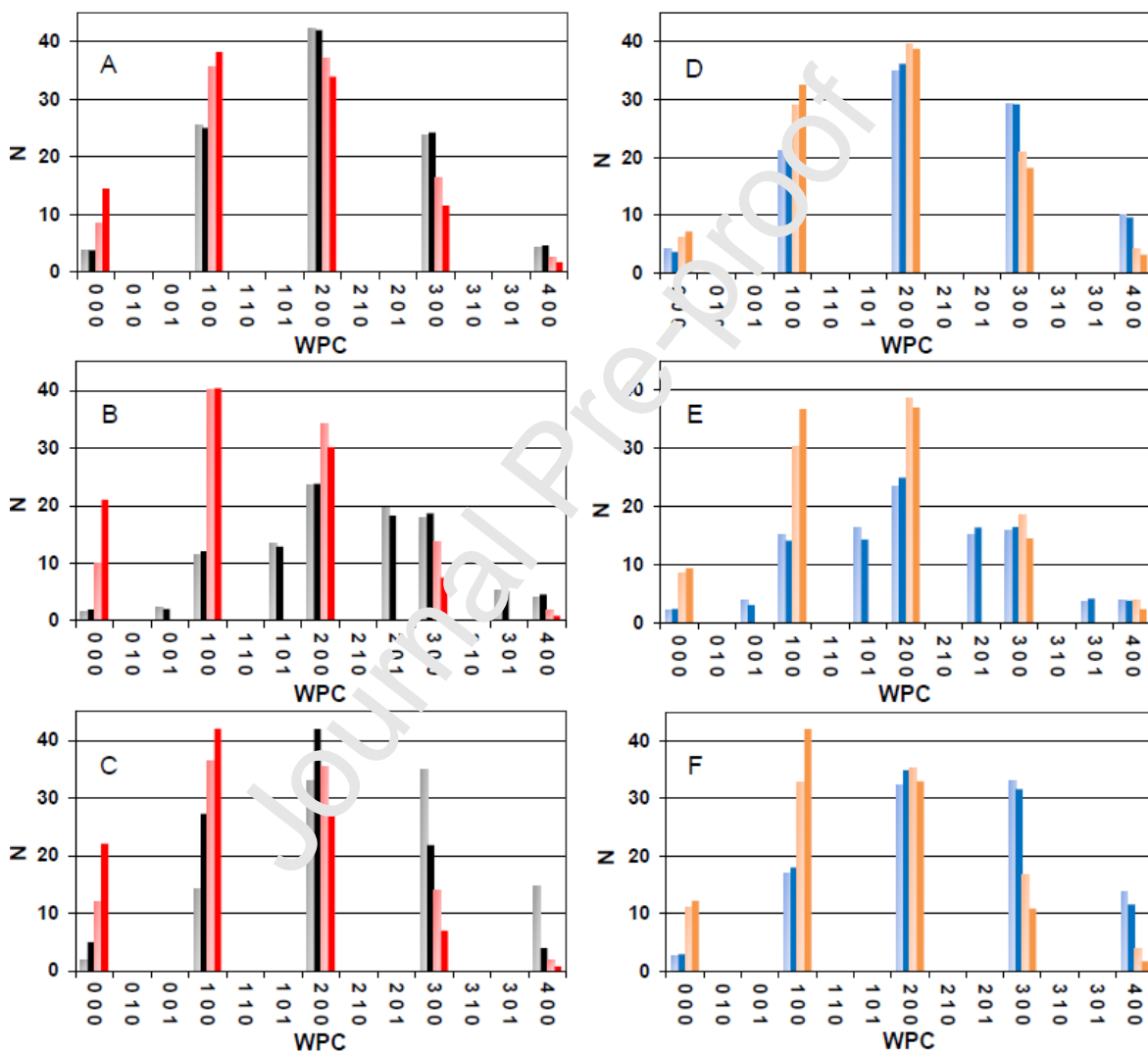


Fig. 6: WPC index for lipid membranes below and above T_m . Fig. A, B and C correspond to DMPC (grey and black) and 14:0 Diether PC membranes (light red and red). Fig. D, E and F correspond to DMPC/Chol (light blue and blue) and 14:0 Diether PC/Chol (light orange and orange) membranes. Top panels

represent the region between PO and CO groups, middle panels represent CO region and bottom panels correspond to acyl chains below CO groups.

In particular, the analysis has been restricted to the region below the phosphate groups in order to highlight the changes around the ester and ether bonds, that is between the PO and CO groups, (panels A and D); the CO group regions itself (panels B and E) and the acyl chains below CO groups (panels C and F).

The index **WPC** represents the number of H-bonds that the water molecules form with other water molecules (W), PO groups (P) and CO groups (C), respectively [37]. For instance, 201 denotes two H-bonds with other water molecules, no H-bonds with PO and one H-bond with CO. This was performed considering all the water molecules at a distance to the lipid heavy atoms lower than 4.5 Å and calculating all their H-bonds with other water molecules, PO and CO groups.

When going from below to above T_m (panels A and B), there are no significant changes in the **WPC** index for DMPC and 14:0 Diether PC in the regions between CO and PO and the CO itself.

In contrast, a significant difference is observed below and above T_m for both lipids in the region between the CO and the acyl chains. In particular, a major increase is observed in the WPC= 000, corresponding to non-bound water molecules which is in accordance with the increase of rotational isomers forming kinks for water appearing at the phase transition [5]. The same behavior was observed for the WPC population 100 (Panel C).

Comparing the behavior of DMPC and 14:0 Diether PC in the same phase states, it is concluded that the absence of CO groups increases the population of

WPC=000. This is congruent with the interpretation that the substitution of an ester bound by an ether one is equivalent to a slight increase in the acyl chain length promoting the same increase in rotational isomers as described for the phase transition [12].

In the three zones, the 14:0 Diether PC membranes exhibit more water molecules without H-bonds (000) and with only one H-bond (100) in comparison with the DMPC membranes, whose water molecules around the lipids form more H-bonds with other water molecules or with the CO atoms. The noticeable increase of the 200 and 300 populations in DMPC membranes denotes that in these lipids the water-water association is increased in comparison to the ether lipids. A similar picture is found above the transition temperature.

The presence of Chol in 14:0 Diether PC and DMPC membranes causes an evident effect on water H-bonds distribution in comparison to pure 14:0 Diether PC and DMPC membranes. For example, 000 and 100 water molecules' populations decrease in 14:0 Diether PC and DMPC membranes with Chol, and the water molecules with two or more H-Bonds increase respect to the pure membranes. This is shown in Fig. 6 for pure 14:0 Diether PC membrane and mixed 14:0 Diether PC/Chol membrane. The same profile is observed above the transition temperature although in an attenuated form.

In this context, DMPC membranes loose population of these class of molecules since there is an increase of water molecules that present a HB with the carbonyl groups of the lipid chains (001, 101, 201 and 301). These molecular classes (which

summed up reach almost 40 percent of the total water molecules in such region) are less prone to relaxation given that they are bound to the lipid chains.

It is well known that the first hydration shell of biomolecules implies both specific and general hydration water. While the former implies bound water (including water molecules hydrogen-bonded to the lipid), the latter involves much weaker interactions (like van der Waals interactions). Thus, the water residence time in the first hydration shell is a result of two well differentiated relaxation behaviors, with the water molecules hydrogen-bonded to the lipid presenting much larger relaxation times. In order to include some dynamical information, the mean residence time the water molecules hydrogen-bonded to the CO of DMPC and the water molecules around the corresponding region of the PC lipids which lack the carbonyl groups, was calculated. To that end, the mean time to abandon the first hydration shell (water molecules in the lipid first neighbors) region, that is to move more than 4.10 angstroms away from the O of the carbonyl of DMPC or the C of the corresponding region of PC lipids was considered. This threshold for the first hydration shell was defined from studies on different systems, ranging from graphene surfaces to proteins, and considering both water density distributions normal to the solute surface (first peak extension) and also distributions of minimum water-solute distances [38–40].

The calculations show that the water molecules hydrogen-bonded to carbonyl groups in DMPC reside within this first hydration shell region 31.2 ps in average, while for 14:0 Diether PC (none water-lipid HB) the timescale is roughly an order of magnitude lower (2.6 ps). Thus, water molecules within the region of the probe for

14:0 Diether PC lipids are much more labile or relaxable than that for DMPC lipids, in accordance with the experimental results

4. Discussion.

In phospholipid vesicles, Laurdan's emission spectra are sensitive to the packing of lipid molecules and consequently to their phase state. A further process that affects Laurdan fluorescence is due to the Molecular Dynamics of water molecules in the vicinity of the probe. For example, the reorientation of water molecule dipoles around the excited-state dipole of Laurdan [9,41].

Comparison of the experiments in Figs 2 and 3 denotes that both the GP_{ex} values and the non-relaxable population are larger in DMPC than 14:0 Diether PC regardless of the phase state. This is because some water molecules form a H-bond with the carbonyl group as confirmed by the MD simulations through the WPC index (Fig. 6). Water is organized around the polar head groups of the lipids forming a bidimensional solution in a region named as "interphase" [42,43]. Under the scope of this work this term has more significant physical meaning than "interface" because this one refers to a mathematical plane dividing the polar and the non-polar region. [44].

The greater organization at the DMPC interphase, can be due to the possibility that water molecules could form an intramolecular water bridge binding simultaneously to PO and CO groups by H bonds, in the same lipid molecule forming a water bridge [13]. The MD results indicate that Chol in DMPC does not break these water bridges, but rather forms a water bridge between CO and its -OH group, giving place to a more ordered interphase region

WPC index reports that the presence of water molecules without H-Bonds (000) or only one H-Bond (100) is higher for 14:0 Diether PC compared to DMPC in accordance with the increase of relaxable population observed by fluorescence analysis (Fig 4 and 6). The addition of Chol to 14:0 Diether PC decreases this population denoted by a lower number of free water molecules.

The intramolecular water bridge is not formed in 14:0 Diether PC due to the absence of CO groups [17]. Hence, the water bound to the PO can rotate around the H-bond given as a result a reorientation of the water dipole increasing the relaxable population. This effect is less noticeable in the presence of Chol suggesting that Chol generates a water bridge between the PO and the -OH group as was reported before [17]. This bridge prevents the rotation of the water molecule bound to the PO, generating a decrease in dipolar relaxation giving place to an increase in GP and non-relaxable population.

At 10% Chol, GP_{ex} values and non-relaxed population in 14:0 Diether PC vesicles are close to those obtained in pure DMPC (Fig 5A and 5B), suggesting that Laurdan is in environments of similar polarities.

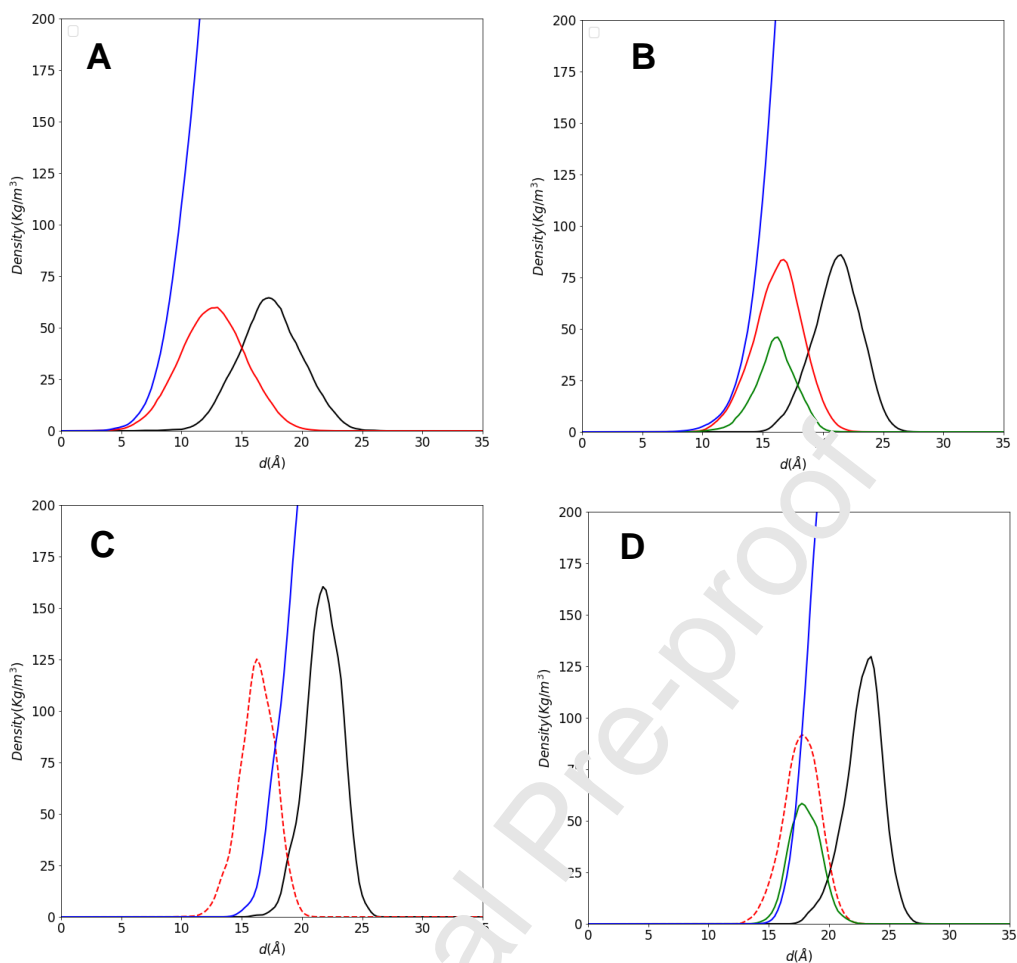


Fig. 7: Density profiles along the Z axis for water (blue line), carbonyl groups (red line), phosphate groups (black line) and cholesterol (green line) for DMPC (A), DMPC/Chol (B), 14:0 Diether PC (C) and 14:0 Diether PC/Chol membranes (D). Dotted red lines in panels (C) and (D) indicate the region where the CO groups should be.

The density profiles shown in Figure 7 indicate that water covers the PO and CO region in DMPC, while in 14:0 Diether PC the CO region where the CO groups should be (dotted lines) and the PO region is displaced to a lower distance with respect to the membrane center. This figure also shows that the -OH group of Chol molecules in 14:0 Diether PC is located in the lipid carbonyl region in the same

position than in DMPC that allow water to penetrate deeper in the mixed membrane. This strongly indicates that Chol is giving water a new residue to bind in the absence of CO.

In order to show the interactions of the water molecules with Chol, a modification of classification index is made. The last digit in the new index, WPCC, considers the H-Bonds with the OH group of the Chol molecules. For example, 2101 denotes two H-Bonds with the OH group of the Chol molecules. For example, 2101 denotes two H-Bonds with other water molecules, one bond with PO from the lipid molecules, no bond with CO lipid groups and one bond with the Chol molecule. In Fig. 8, it is noted that water molecules bound to other water molecules and Chol (1001 and 2001) prevail in both lipid mixtures. The absence of the carbonyl groups implies an increase in the number of water molecules bonded to PO groups and Chol (0101 and 1101).

In a previous work, it was shown that the -OH group of Chol in ether PC is able to bind to the PO group [17].

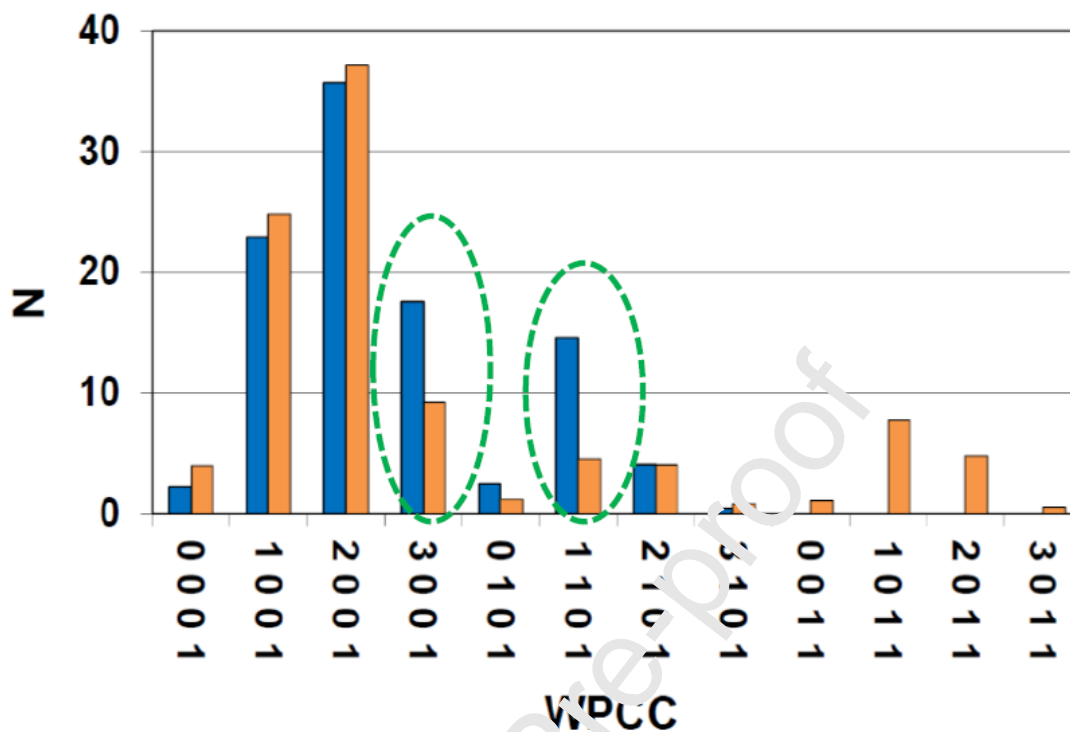


Fig. 8: WPC index for water molecules in 14:0 Diether PC/Chol (blue) and DMPC/Chol membranes (orange).

In correlation with this organization imposed by Chol, a further inspection of Figure 6, indicates that the distributions of WPC index of pure DMPC below T_m 000; 100; 200; 300 and 400, are nearly coincident to those found for 14:0 Diether PC with cholesterol in the region of PO/CO groups. This explains why the GP_{ex} values for these two membranes are coincident in 0.4 as shown in Figure 2, strongly supporting that the probe is laying in this region. The point that the sharp transition is visualized in Figures 1 and 2 at around 10% Chol suggests that the required association needed to give this interfacial property is formed in a specific ratio of 14:0 DietherPC/Chol.

5. Conclusion

Regardless the phase state, the presence of Chol both in DMPC and 14:0 Diether PC vesicles, changed the distribution of water molecules decreasing the dipole relaxation of the lipid interphase generating an increase in the non-relaxable population. These results are corroborated with the WPC index obtained by MD analysis.

The simulations made evident the fact that the addition of Chol in DMPC membranes reduces the amount of labile (that is, easily relaxable hydration water) at expense of an increase of water molecules hydrogen bonded to the lipid carbonyls. These water molecules, which are sensed by Laurdan GP, exhibit a local residence time roughly one order of magnitude larger than the corresponding one for ether PC lipids.

The comparison of the effects of Chol on DMPC and 14:0 Diether PC membrane model systems, indicates that at the molecular level, Chol generate anomalies in interfacial properties of membrane due to different water arrangements. On one hand, it interacts differently with the PO group if CO groups are present or not due to the formation of water bridges. Another important observation in this work is that Chol is able to conform a new hydration site for water in membranes lacking carbonyl groups.

Ether lipids and its mixture with Chol contribute to the stabilization of lipid raft microdomains involve in cellular signaling in particular the water distribution at the interphase may provide structural characteristic affecting membrane fusion and dynamics. The present studies in DMPC/ 14:0 Diether PC /Chol indicate in a first

attempt that the incorporation of ether linked acyl chains in phospholipids affect the response of membrane by modifying intermolecular hydrogen bonds between the head groups [16].

Supplementary Figures

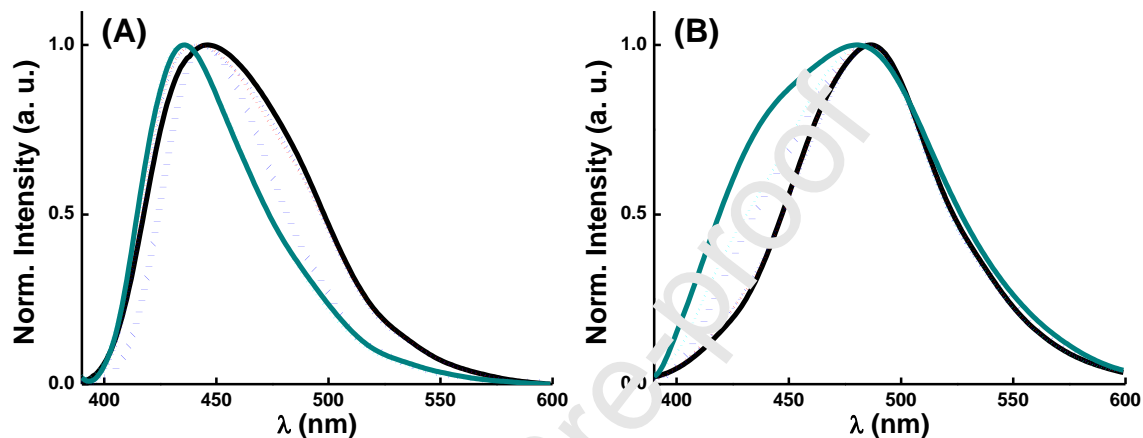


Fig. S1: 14:0 Diether PC normalized Laurdan emission spectra below (A) and above (B) T_m at increasing cholesterol concentrations from 0 (black line) to 30% (green line). Blue dotted lines show the normalized Laurdan emission spectra for DMPC in both conditions.

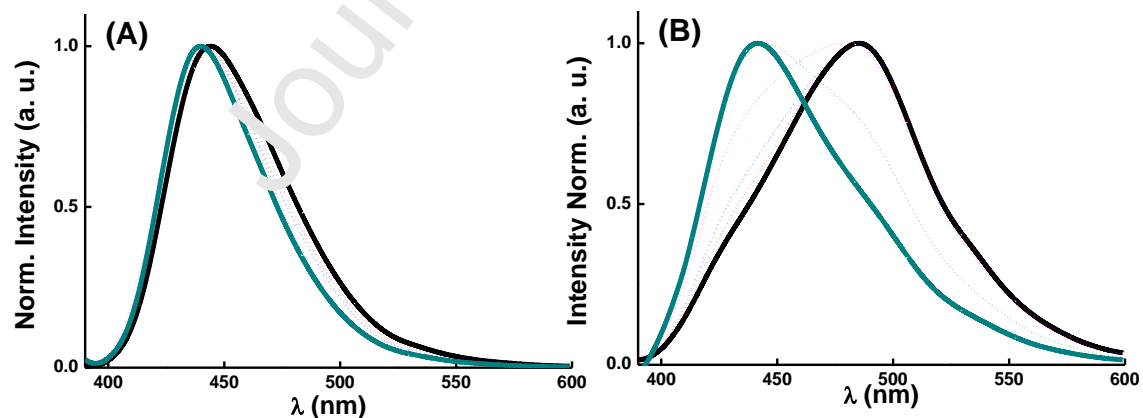


Fig. S2: DMPC normalized Laurdan emission spectra below (A) and above T_m (B) at increasing cholesterol concentrations from 0 (black line) to 30% (green line).

References.

- [1] N.J. Munn, E. Arnio, D. Liu, R.A. Zoeller, L. Liscum, Deficiency in ethanolamine plasmalogen leads to altered cholesterol transport, *J. Lipid Res.* 44 (2003) 182–192. <https://doi.org/10.1194/jlr.M200363-JLR200>.
- [2] K. Gorgas, A. Teigler, D. Komljenovic, W.W. Just, The ether lipid-deficient mouse: Tracking down plasmalogen functions, *Biochim. Biophys. Acta - Mol. Cell Res.* 1763 (2006) 1511–1526. <https://doi.org/10.1016/j.bbamcr.2006.08.038>.
- [3] R.M. Epand, Cholesterol and the interaction of proteins with membrane domains, *Prog. Lipid Res.* 45 (2006) 279–294. <https://doi.org/10.1016/j.plipres.2006.02.001>.
- [4] H. Heerklotz, A. Tsamaloukas, Gradual Change or Phase Transition: Characterizing Fluid Lipid-Cholesterol Membranes on the Basis of Thermal Volume Changes, *Biophys. J.* 91 (2006) 600–607. <https://doi.org/10.1529/biophysj.106.082669>.
- [5] E.A. Disalvo, O.A. Pinto, M.F. Martini, A.M. Bouchet, A. Hollmann, M.A. Frías, Functional role of water in membranes updated: A tribute to Träuble, *Biochim. Biophys. Acta - Biomembr.* 1848 (2015) 1552–1562. <https://doi.org/10.1016/j.bbamem.2015.03.031>.
- [6] D. Marsh, Liquid-ordered phases induced by cholesterol: A compendium of binary phase diagrams, *Biochim. Biophys. Acta - Biomembr.* 1798 (2010) 688–699. <https://doi.org/10.1016/j.bbamem.2009.12.027>.
- [7] L.A. Bagatolli, Monitoring Membrane Hydration with 2-(Dimethylamino)-6-Acylnaphthalenes Fluorescent Probes, in: *Membr. Hydration*, Springer, 2015: pp. 105–125. https://doi.org/10.1007/978-3-319-19060-0_5.
- [8] T. Parasassi, M. Di Stefano, M. Loiero, G. Ravagnan, E. Gratton, Cholesterol modifies water concentration and dynamics in phospholipid bilayers: a fluorescence study using Laurdan probe, *Biophys. J.* 66 (1994) 763–768. [https://doi.org/10.1016/S0006-3495\(94\)80852-5](https://doi.org/10.1016/S0006-3495(94)80852-5).
- [9] H.A. Pérez, A. Disalvo, M. de los Á. Frías, Effect of cholesterol on the surface polarity and hydration of lipid interphases as measured by Laurdan fluorescence: New insights, *Colloids Surfaces B Biointerfaces.* 178 (2019) 346–351. <https://doi.org/10.1016/j.colsurfb.2019.03.022>.
- [10] J.A. Mondal, S. Nihonyanagi, S. Yamaguchi, T. Tahara, Three Distinct Water Structures at a Zwitterionic Lipid/Water Interface Revealed by Heterodyne-Detected Vibrational Sum Frequency Generation, *J. Am. Chem. Soc.* 134 (2012) 7842–7850. <https://doi.org/10.1021/ja300658h>.

- [11] E.A. Disalvo, F. Lairion, F. Martini, E. Tymczyszyn, M. Frías, H. Almaleck, G.J. Gordillo, Structural and functional properties of hydration and confined water in membrane interfaces, *Biochim. Biophys. Acta - Biomembr.* 1778 (2008) 2655–2670. <https://doi.org/10.1016/j.bbamem.2008.08.025>.
- [12] A.S. Rosa, J.P. Cejas, E.A. Disalvo, M.A. Frías, Correlation between the hydration of acyl chains and phosphate groups in lipid bilayers: Effect of phase state, head group, chain length, double bonds and carbonyl groups, *Biochim. Biophys. Acta - Biomembr.* 1861 (2019) 1197–1203. <https://doi.org/10.1016/j.bbamem.2019.03.018>.
- [13] H.A. Pérez, J.P. Cejas, A.S. Rosa, R.E. Giménez, E.A. Disalvo, M.A. Frías, Modulation of Interfacial Hydration by Carbonyl Groups in Lipid Membranes, *Langmuir.* 36 (2020) 2644–2653. <https://doi.org/10.1021/acs.langmuir.9b03551>.
- [14] N. Watanabe, K. Suga, J.P. Slotte, T.K.M. Nyholm, H. Umakoshi, Lipid-Surrounding Water Molecules Probed by Time-Resolved Emission Spectra of Laurdan, *Langmuir.* 35 (2019) 9b00303. <https://doi.org/10.1021/acs.langmuir.9b00303>.
- [15] T. Parasassi, G. De Stasio, G. Ravagnan, R.M. Rusch, E. Gratton, Quantitation of lipid phases in phospholipid vesicles by the generalized polarization of Laurdan fluorescence, *Biophys. J.* 60 (1991) 179–189. [https://doi.org/10.1016/S0006-3495\(91\)82041-0](https://doi.org/10.1016/S0006-3495(91)82041-0).
- [16] J.M. Dean, I.J. Lodhi, Structural and functional roles of ether lipids, *Protein Cell.* 9 (2018) 196–206. <https://doi.org/10.1007/s13238-017-0423-5>.
- [17] J. Pan, X. Cheng, F.A. Heberle, B. Mostofian, N. Kučerka, P. Drazba, J. Katsaras, Interactions between Ether Phospholipids and Cholesterol As Determined by Scattering and Molecular Dynamics Simulations, *J. Phys. Chem. B.* 116 (2012) 14829–14838. <https://doi.org/10.1021/jp310345j>.
- [18] P.L.-G. Cheng, P.T.T. Wong, Interactions of Laurdan with phosphatidylcholine liposomes: a high pressure FTIR study, *Biochim. Biophys. Acta - Biomembr.* 1149 (1993) 260–266. [https://doi.org/10.1016/0005-2736\(93\)90209-I](https://doi.org/10.1016/0005-2736(93)90209-I).
- [19] A.D. Bangham, M.W. Hill, N.G.A. Miller, Preparation and Use of Liposomes as Models of Biological Membranes, in: *Methods Membr. Biol.*, Springer US, Boston, MA, 1974: pp. 1–68. https://doi.org/10.1007/978-1-4615-7422-4_1.
- [20] N.J. Cho, L.Y. Hwang, J.J.R. Solandt, C.W. Frank, Comparison of extruded and sonicated vesicles for planar bilayer self-assembly, *Materials (Basel).* 6 (2013) 3294–3308. <https://doi.org/10.3390/ma6083294>.
- [21] J.R. Lakowicz, *Principles of fluorescence spectroscopy*, Springer science &

business media, 2013.

- [22] J.D. Nickels, J. Katsaras, Water and Lipid Bilayers, in: *Membr. Hydration*, Springer, 2015: pp. 45–67. https://doi.org/10.1007/978-3-319-19060-0_3.
- [23] T. Parasassi, M. Di Stefano, M. Loiero, G. Ravagnan, E. Gratton, Influence of cholesterol on phospholipid bilayers phase domains as detected by Laurdan fluorescence, *Biophys. J.* 66 (1994) 120–132. [https://doi.org/10.1016/S0006-3495\(94\)80763-5](https://doi.org/10.1016/S0006-3495(94)80763-5).
- [24] M. Bacalum, B. Zorila, M. Radu, Fluorescence spectra decomposition by asymmetric functions: Laurdan spectrum revisited, *Anal. Biochem.* 440 (2013) 123–129. <https://doi.org/10.1016/j.ab.2013.05.031>.
- [25] K.J. Millman, M. Aivazis, Python for Scientists and Engineers, *Comput. Sci. Eng.* 13 (2011) 9–12. <https://doi.org/10.1109/MCSE.2011.36>.
- [26] W. McKinney, others, Data structures for statistical computing in python, in: *Proc. 9th Python Sci. Conf.*, 2010: pp. 51–53.
- [27] S. van der Walt, S.C. Colbert, G. Varoquaux, The NumPy Array: A Structure for Efficient Numerical Computation, *Comput. Sci. Eng.* 13 (2011) 22–30. <https://doi.org/10.1109/MCSE.2011.37>.
- [28] S. Jo, J.B. Lim, J.B. Klauda, W. Im, CHARMM-GUI Membrane Builder for Mixed Bilayers and Its Application to Yeast Membranes, *Biophys. J.* 97 (2009) 50–58. <https://doi.org/10.1016/j.bpj.2009.04.013>.
- [29] D.A. Case, R.M. JTB, D.S. Betz, T.E. Cerutti III, T.A. Cheatham III, R.E. Darden, Duke, T.J. Giese, H. Gohlke, AW Goetz, N. Homeyer, S. Izadi, P. Janowski, J. Kaus, A. Kovalenko, TS Lee, S. LeGrand, P. Li, T. Luchko, R. Luo, B. Madej, KM Merz, G. Monard, P. Needham, H. Nguyen, HT Nguyen, I. Omelyan, A. Onufriev, DR Roe, A. Roitberg, R. Salomon-Ferrer, CL S. (2015).
- [30] I. Gould, A. Skjevik, C. Dickson, B. Madej, R. Walker, Lipid17: A Comprehensive AMBER Force Field for the Simulation of Zwitterionic and Anionic Lipids, *Manuscr. Prep.* (2018).
- [31] J. Wang, R.M. Wolf, J.W. Caldwell, P.A. Kollman, D.A. Case, Development and testing of a general amber force field, *J. Comput. Chem.* 25 (2004) 1157–1174. <https://doi.org/10.1002/jcc.20035>.
- [32] W.H. Press, S.A. Teukolsky, W.T. Vetterling, B.P. Flannery, *Numerical recipes 3rd edition: The art of scientific computing*, Cambridge university press, 2007. <https://books.google.es/books?hl=es&lr=&id=1aAOdzK3FegC&oi=fnd&pg=PA1&dq=Numerical+recipes+3rd+edition:+The+art+of+scientific+computing&ots=3kVnHaAmqh&sig=QT2Qwvq48GRo6F5tRVUD->

41LGQQ#v=onepage&q=Numerical recipes 3rd edition%3A The art of scientific compu.

- [33] R.W. Pastor, B.R. Brooks, A. Szabo, An analysis of the accuracy of Langevin and molecular dynamics algorithms, *Mol. Phys.* 65 (1988) 1409–1419. <https://doi.org/10.1080/00268978800101881>.
- [34] H.J.C. Berendsen, J.P.M. Postma, W.F. van Gunsteren, A. DiNola, J.R. Haak, Molecular dynamics with coupling to an external bath, *J. Chem. Phys.* 81 (1984) 3684–3690. <https://doi.org/10.1063/1.448118>.
- [35] T. Darden, D. York, L. Pedersen, Particle mesh Ewald: An $N \cdot \log(N)$ method for Ewald sums in large systems, *J. Chem. Phys.* 98 (1993) 10089–10092. <https://doi.org/10.1063/1.464397>.
- [36] T. Parasassi, G. De Stasio, A. D’Ubaldo, E. Gratton, Phase fluctuation in phospholipid membranes revealed by Laurdan fluorescence, *Biophys. J.* 57 (1990) 1179–1186. [https://doi.org/10.1016/S006-3495\(90\)82637-0](https://doi.org/10.1016/S006-3495(90)82637-0).
- [37] L.M. Alarcón, M. de los Angeles Frías, M.A. Morini, M. Belén Sierra, G.A. Appignanesi, E. Anibal Disalvo, Water populations in restricted environments of lipid membrane interphases, *Eur. Phys. J. E.* 39 (2016) 94. <https://doi.org/10.1140/epje/i2016-16094-5>.
- [38] D.C. Malaspina, E.P. Schulz, L.M. Alarcón, M.A. Frechero, G.A. Appignanesi, Structural and dynamical aspects of water in contact with a hydrophobic surface, *Eur. Phys. J. E.* 32 (2010) 35–42. <https://doi.org/10.1140/epje/i2010-10594-2>.
- [39] L.M. Alarcón, D.C. Malaspina, E.P. Schulz, M.A. Frechero, G.A. Appignanesi, Structure and orientation of water molecules at model hydrophobic surfaces with curvature: From graphene sheets to carbon nanotubes and fullerenes, *Chem. Phys.* 388 (2011) 47–56. <https://doi.org/10.1016/j.chemphys.2011.07.019>.
- [40] S.R. Accornero, D.C. Malaspina, J.A. Rodríguez Fris, L.M. Alarcón, G.A. Appignanesi, Temperature dependence of the structure of protein hydration water and the liquid-liquid transition, *Phys. Rev. E.* 85 (2012) 031503. <https://doi.org/10.1103/PhysRevE.85.031503>.
- [41] T. Parasassi, G. Ravagnan, R.M. Rusch, E. Gratton, Modulation and Dynamics of Phase Properties in Phospholipid Mixtures Detected By Laurdan Fluorescence, *Photochem. Photobiol.* 57 (1993) 403–410. <https://doi.org/10.1111/j.1751-1097.1993.tb02309.x>.
- [42] S. Damodaran, Water activity at interfaces and its role in regulation of interfacial enzymes, *Colloids Surfaces B Biointerfaces.* 11 (1998) 231–237. [https://doi.org/10.1016/S0927-7765\(98\)00040-X](https://doi.org/10.1016/S0927-7765(98)00040-X).

- [43] E.A. Disalvo, A. Hollmann, M.F. Martini, Hydration in Lipid Monolayers: Correlation of Water Activity and Surface Pressure, in: *Membr. Hydration*, Springer, 2015: pp. 213–231. https://doi.org/10.1007/978-3-319-19060-0_9.
- [44] T.J. McIntosh, S.A. Simon, J.P. Dilger, Location of the water-hydrocarbon interface in lipid bilayers, *Water Transp. Biol. Membr.* 1 (1989) 1–15.

Journal Pre-proof

Declaration of interests

The authors declare that they have no known competing financial interests or personal relationships that could have appeared to influence the work reported in this paper.

The authors declare the following financial interests/personal relationships which may be considered as potential competing interests:

Journal Pre-proof

Santiago del Estero, May 1st, 2020

To the Executive Editor,

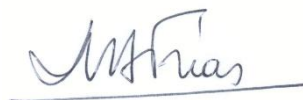
Dr. Hans Vogel

BBActa-Biomembranes

The authors of the paper **EFFECT OF CHOLESTEROL ON THE HYDRATION PROPERTIES OF ESTER AND ETHER LIPID MEMBRANE INTERPHASES.**

by H.A. Pérez, L.M. Alarcón, A.P. Verde, G.A. Appignanesi, R.E. Giménez, E.A. Disalvo, and myself, which is submitted for publication in BBA Biomembranes declare no conflicts of interest

Sincerely



Dr. Maria A. Frias

National Council for Scientific and Technical

Research